High-performance 459-nm Cs Cell Optical Frequency Standard with a Predicted Frequency Stability of 10^{-14}

Jia Zhang, Jianxiang Miao, Tiantian Shi, and Jingbiao Chen
State Key Laboratory of Advanced Optical Communication Systems and Networks, School of Electronics
Peking University
Beijing, China
tts@pku.edu.cn

***Summary*—In order to achieve a high-performance 459-nm Cs cell optical frequency standard, its frequency is locked by modulation transfer spectroscopy with power stabilized using an acousto-optic modulator. The power-stabilized operation can optimize the frequency stability caused by power fluctuations. To reduce the common-mode noise of two independent systems, we use a "dual optical path" scheme to lock the frequencies of two independent systems to one Cs atomic vapor cell. In addition, the optical components of the whole system are fixed on a silica baseboard to reduce the influence caused by vibration and thermal expansion. Our proposed scheme is expected to achieve an optical frequency standard with frequency stability of 10^{-14} level. This high-stability optical frequency standard has promising applications in fundamental physics research and laser spectroscopy.**

***Keywords*—optical clock; optical frequency standard; power-stabilization**

I. Introduction

Atomic clocks with high stability are widely used in many fields, such as space exploration [1], basic physics research [2], and so on. For applications with less stringent requirements on clock performance, there are significant advantages using a thermal atomic cell as the quantum reference because of its better compactness and portability. Among them, the modulation transfer spectroscopy (MTS) technique [3,4] is often used because of the large-slope error signal, insensitivity to background absorption, and rejection of low-frequency noise. Currently, there are various experimental schemes based on MTS stabilization, such as 852-nm Cs [5], 459-nm Cs [6], 420-nm Rb [7], and 532-nm I_2 [8] optical frequency standards.

At present, the self-estimated frequency stability of MTS-stabilized 459-nm laser reaches $1.4 \times 10^{-14}/\sqrt{\tau}$ and the Allan deviation measured via beat detection achieves $2.1 \times 10^{-13}/\sqrt{\tau}$ experimentally [6]. However, in our previous experiment, we found that the relative intensity noise (RIN) of the laser gets worse after performing the frequency stabilization. It has been shown that power fluctuations at high frequencies can reduce the signal-to-noise ratio, degrading the short-term frequency stability [9]. Low-frequency fluctuations in power can affect long-term stability [10]. In short, the power fluctuations will inevitably affect the stability. Therefore, to achieve a high-stability optical frequency standard, it is necessary to perform power stabilization.

Experimentally, there are usually two types of schemes, internal and external modulation, to achieve power stabilization. Internal modulation refers to the stabilization of laser power by adjusting the laser's internal feedback, such as the resonant cavity length, diode current, or temperature. However, internal modulation often comes at the expense of frequency stability and is therefore not suitable for building high-stability optical frequency standards. External modulation refers to the establishment of a power feedback loop outside the laser. For example, adding optical modulation devices such as electro-optic modulator [11], acousto-optic modulator (AOM) [12,13], or photo-elastic modulator [14] to the external optical path to form a control loop with the feedback devices, thus realize the amplitude modulation of the laser. Compared with internal modulation, external modulation can stabilize the power without changing the frequency, providing a good choice for building a high-stability 459-nm Cs cell optical frequency standard.

Here, we use AOMs to stabilize the laser power while locking the laser frequency of the two systems to the Cs atom 459-nm $6S_{1/2}$-$7P_{1/2}$ transition. To reduce the common-mode noise of the two 459-nm optical frequency standards, we lock the frequencies of two system to one vapor cell. In addition, the optical components of the whole system are fixed on a silica baseboard to reduce the impact due to thermal expansion, vibration, and other factors. This scheme is expected to achieve higher frequency stability of the 459-nm Cs cell optical frequency standard, which can be used as a pumping source to achieve higher performance Cs four-level active optical clock (AOC) [15,16].

II. Methods

The scheme of the high-performance 459-nm Cs cell optical frequency standard is shown in Fig. 1. In our proposed experimental scheme, a home-made 459-nm interference filter configuration external cavity diode laser (IF-ECDL) is used as the local oscillator. The optical part of the whole system is divided into three modules: the power stabilization module, the frequency stabilization module, and the beat detection module. All components are fixed on a silica baseboard to reduce the effects of thermal expansion, vibration, and other factors. Since the polarization of the laser has an effect on the power stability, the laser first passes through a Glan-Taylor (GT) prism for consistent adjustment of the polarization direction, and then through a half-wave plate (HWP) and an AOM. Passing through the AOM, first-order diffraction beams are diverted from the zeroth-order. For easy adjustment of the subsequent optical path, the zeroth-order light is used as the power-stabilized output. Here, a small aperture diaphragm is needed to allow only zeroth-order light to pass through. The zeroth-order light is divided into two parts by the combination of a HWP and a PBS, one of which enters the frequency stabilization module. The other part is again divided into two beams through a combination of a HWP and a PBS. One beam enters the photodetector to convert the light signal into an electrical signal, yielding an error signal back to the driver side of the AOM. The diffraction efficiency of the AOM is adjusted by changing the magnitude of the modulation signal applied to the AOM, which in turn changes the power value of the zeroth-order light. When the voltage value corresponding to the reflected light is equal to the reference voltage setting, the

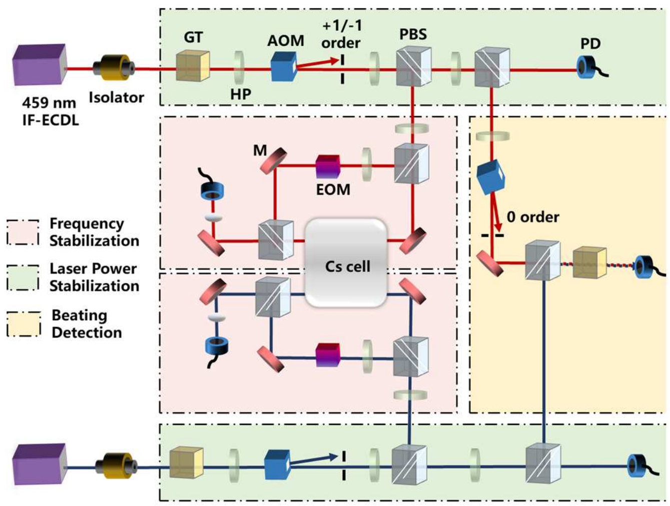

(a)

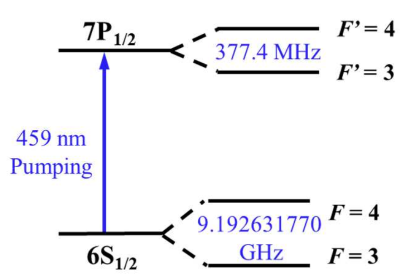

(b)

Figure 1. (a) The schematic of the high-performance 459-nm Cs cell optical frequency standard. 459-nm IF-ECDL, 459-nm interference filter configuration external cavity diode laser; GT, Glan-Taylor prism; HWP, half wavelength plate; AOM, acoustic optical modulator; PBS, polarization beam splitter; EOM, electro-optical modulator; FC, fiber coupler; M, reflecting mirror; PD, photodetector. (b) The hyperfine levelsof the Cs 6S1/2 and 7P1/2 energy levels.

power locking is achieved.

Through MTS, we lock the two 459-nm IF-ECDLs both to the Cs atom 459 nm $6S_{1/2}$-$7P_{1/2}$ transition. For each system, the laser entering the frequency stabilization module is divided into probe and pump beams. The pump light is phase-modulated by the EOM and then overlaps with the probe light in the Cs cell at a lin⊥lin counter-propagating configuration. After four-wave mixing processes, the modulated signal is transferred to the probe light. The error signal is obtained after mixing and demodulation. This error signal is then sent to the PID locking system in order to stabilize the output frequency of the ECDL. It should be noted that the two systems share one Cs atomic cell for frequency locking, which will largely reduce the influence of common-mode noise on beating signal. It is expected that the beating frequency stability can be improved by one order of magnitude, reaching the same order of magnitude (10^{-14}) as the self-estimated value.

III. RESULTS

Experimentally, we use the MTS to perform frequency locking of the 459-nm laser. In the frequency stabilization module, the modulated signal applied to the pump light by the EOM is transferred to the probe light, and after demodulation, a dispersionlike error signal can be obtained for frequency stabilization. We use PID servo circuit to feedback the error signal to different ports of the laser and control the output frequency of the laser in real time to achieve closed-loop locking of the whole system.

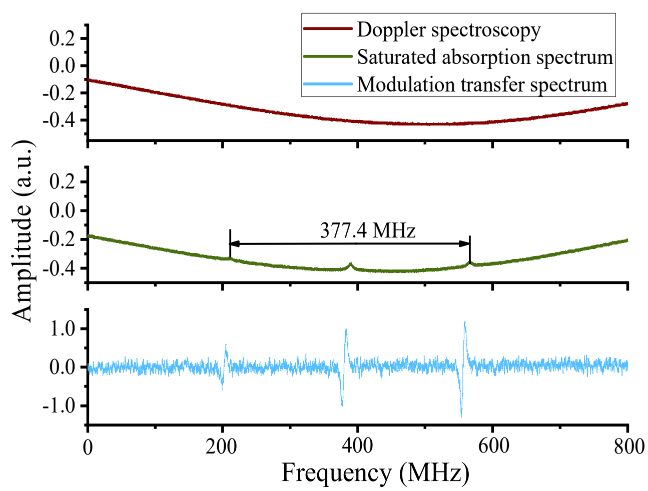

Figure 2. The Doppler spectroscopy, saturated absorption spectrum, and modulation transfer spectrum observed in the experiment.

After achieving the initial lock, we evaluate the frequency stability based on the fluctuation of the remaining error signal, which is a common method to evaluate the stability of optical frequency internationally. The Doppler spectroscopy, saturated absorption spectrum (SAS), and MTS observed in the experiment are shown in Fig. 2. The SAS corresponds to the three peaks of the two hyperfine energy levels $F = 3$ and $F = 4$ of the Cs atom and their crossover. The frequency spacing between the two hyperfine energy levels $F = 3$ and $F = 4$ is 377.4 MHz, which can be calibrated the MTS slope.

When locking, the laser will be locked at the zero-crossing point of the MTS, so its slope is an important reference indicator of the system parameters. The higher the slope and the larger the amplitude, the better the signal-to-noise ratio and the better the locking effect. There are many factors affecting the final stability, including: the power of the pump light and probe light, modulation frequency, modulation amplitude, and vapor cell temperature. Referring to the previous experimental data, the power of the pump light and probe light are set to 1.2 mW and 0.2 mW, respectively. We measured the MTS slope and amplitude at different vapor cell temperatures and modulation frequencies to find the optimal operating conditions, as shown in Figs 3(a) and 3(b). As the cell temperature increases, the MTS slope first increases and then decreases; The amplitude and slope changes are similar. For the comprehensive consideration of the MTS slope and the MTS amplitude, 112℃ is selected as the optimal working temperature point. When the modulation frequency is 1.68 MHz, the MTS slope reaches its maximum value, and the peak-to-peak value of the error signal

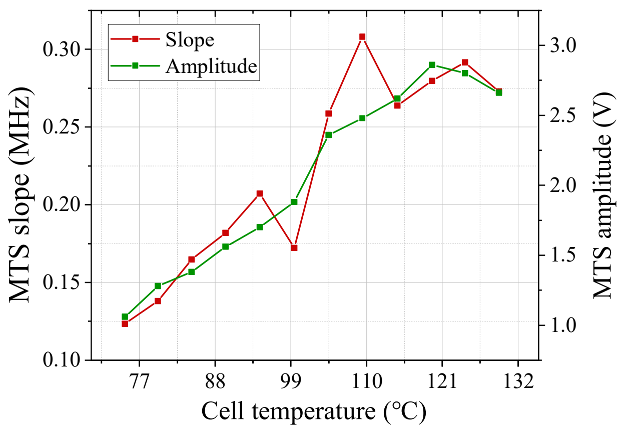

(a)

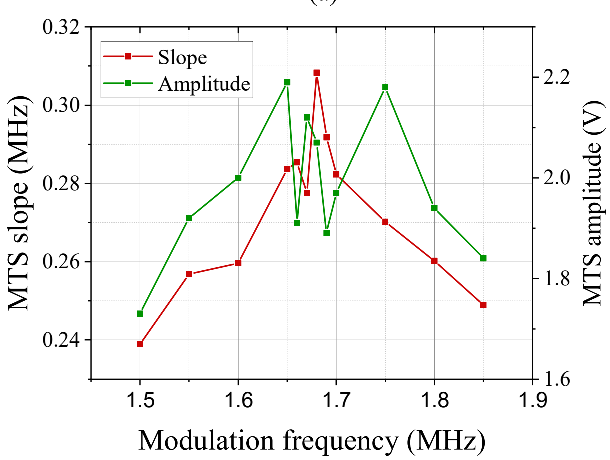

(b)

Figure 3. (a) MTS signal slope and amplitude at zero crossing, measured at cell temperatures. (b) MTS signal slope and amplitude at zero crossing, measured at different modulation frequencies.

is 2.07 V. Therefore, the optimal setting value for modulation frequency at 1.68 MHz will be carried out in this experiment.

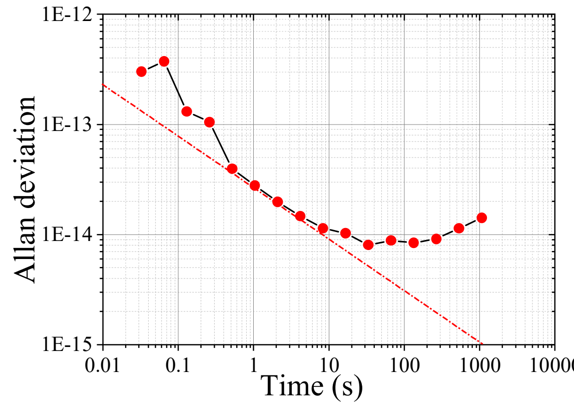

(a)

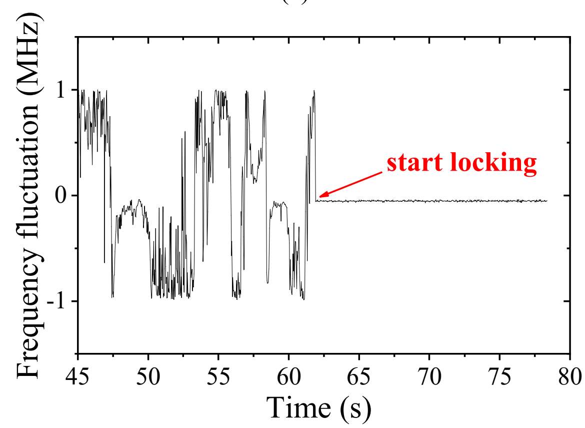

(b)

Figure 4. (a) Allan deviation of the 459-nm laser stabilized via MTS, measured by self-estimation. The short-term stability measured at averaging time of 1 s is 2.8×10-14. (b) Comparison of MTS error signals before and after locking.

By optimizing the feedback gain, the short-term stability measured with self-estimation at averaging time of 1 s is 2.8×10^{-14}, reaching 10^{-15} at 20-s averaging time, as shown in Figure 4(a). The frequency stabilization can also be seen by comparing the frequency fluctuations before and after locking in Fig. 4(b). When the laser is running freely, the frequency fluctuation range of the error signal is about 2 MHz. After frequency stabilization using MTS, the fluctuation range is reduced by two orders of magnitude. The comparison shows that the fluctuations of the error signal are greatly suppressed after locking. The small fluctuations in the residual error signal may be caused by small fluctuations in the laboratory temperature, the cell temperature, and vibrations. In the next step, we will further optimize the frequency stabilization and perform power stabilization for both sets of lasers, to achieve the same level of beating frequency stability as the self-estimation.

IV. DISCUSSION

Our proposed high-stability 459-nm Cs cell optical frequency standard is further power stabilized on the basis of frequency stabilization. The power-stabilized operation can reduce the frequency instability caused by power fluctuations and improve the performance of the optical frequency standard.

Experimentally, we will optimize the power stability by measuring RIN and compare the frequency stability before and after power stabilization to obtain the specific effect of power fluctuations. In our previous experiments, we found that the beating frequency stability of two independent systems was nearly one order of magnitude worse than the self-estimated value. To reduce the effect of the common-mode noise, we lock the frequencies of two independent 459-nm lasers to the same Cs atomic cell, which can greatly reduce the effect on the stability caused by the temperature fluctuations of different cells. Moreover, the optical components of the complete system are fixed in a silica baseboard, which can largely weaken the impact caused by vibration, and thermal expansion. Overall, the frequency stability is expected to be optimized in one order of magnitude, reaching a small factor of 10^{-14} at 1 s. If this high-stable 459-nm laser is used as the pump source for Cs four-level AOC, the linewidth of the clock laser will also be narrowed.

V. Conclusions

We propose a scheme to reduce the common-mode noise by locking two independent 459-nm lasers to one Cs atomic vapor cell. While performing MTS frequency stabilization, AOMs are used to stabilize the laser power. To reduce the effects of thermal expansion, vibration, etc., the whole system uses silica as the baseboard. In addition to being used as an optical frequency standard, this high-stability 459-nm laser can be used as a pumping laser to achieve higher performance Cs four-level AOC.

Acknowledgment

This work was supported by the Innovation Program for Quantum Science and Technology (2021ZD0303200), China Postdoctoral Science Foundation (BX2021020), and Wenzhou Major Science and Technology Innovation Key Project (ZG2020046).

References

[1] S. Kolkowitz, et al. "Gravitational wave detection with optical lattice atomic clocks." Phys. Rev. D., vol. 94, no. 12, pp. 124043, 2016.

[2] R. M. Godun, et al. "Frequency ratio of two optical clock transitions in $^{171}Yb^{+}$ and constraints on the time variation of fundamental constants." Phys. Rev. Lett., vol. 113, no. 21, pp. 210801, 2014.

[3] B. Wu, et al. "Modulation transfer spectroscopy for D1 transition line of rubidium." JOSA B., vol. 35, no. 11, pp. 2705-2710, 2018.

[4] F. Zi, et al. "Laser frequency stabilization by combining modulation transfer and frequency modulation spectroscopy." Appl. Opt., vol. 56. no. 10. pp. 2649-2652, 2017.

[5] H. Shi, et al. "Frequency Stabilization of a Cesium Faraday Laser with a double-layer vapor cell as frequency reference." IEEE Photonics J., vol.14, no.6, pp.1-6, 2022.

[6] J. Miao, et al. "Compact 459-nm Cs cell optical frequency standard with $2.1 \times 10^{-13}/\sqrt{\tau}$ short-term stability." Phys. Rev. Appl., vol. 18, no. 2, pp. 024034, 2022.

[7] P. Chang, et al. "Stabilizing diode laser to 1 Hz-level Allan deviation with atomic spectroscopy for Rb four-level active optical frequency standard." Appl. Phys. B., vol. 125, no. 11, pp. 196, 2019.

[8] T. Schuldt, et al. "Development of a compact optical absolute frequency reference for space with 10^{-15} instability." Appl. Opt., vol. 56, no. 4, pp. 1101-1106, 2017.

[9] M. Abdel Hafiz, et al. "A high-performance Raman-Ramsey Cs vapor cell atomic clock." J. Appl. Phys., vol. 121, no. 10, pp. 104903, 2017.

[10] O. Kozlova, et al. "Limitations of long-term stability in a coherent population trapping Cs clock." IEEE Trans. Instrum. Meas., vol. 63, no. 7, pp. 1863-1870, 2014.

[11] F. Liu, et al. "Long-term and wideband laser intensity stabilization with an electro-optic amplitude modulator." Opt. Laser Technol., vol. 45, pp. 775-781, 2013.

[12] F. Tricot, et al. "Power stabilization of a diode laser with an acousto-optic modulator." Rev. Sci. Instrum., vol. 89, no. 11, pp. 113112, 2018.

[13] V. I. Balakshy, et al. "Dynamic processes in an acousto-optic laser beam intensity stabilization system." Opt. Laser Technol., vol. 62, pp.89-94, 2014.

[14] L. Duan, et al. "Light intensity stabilization based on the second harmonic of the photoelastic modulator detection in the atomic magnetometer." Opt. Express, vol. 23, no. 25, pp. 32481-32489, 2015.

[15] T. Shi, et al. "Realization of phase locking in good-bad-cavity active optical clock." Opt. Express, vol. 27, no. 16, pp. 22040-22052, 2019.

[16] T. Shi, et al. "An inhibited laser." Commun. Phys., vol. 5, no. 1, pp. 1-10, 2022.